Cellulose (2024) 31:953–967
https://doi.org/10.1007/s10570-023-05573-2

ORIGINAL RESEARCH

Fenton-like oxidation of pinewood to produce cellulose nanoparticles in one pot treatment

Poornima Vijay · Vikram Singh Raghuwanshi · Jisheng Ma · Warren Batchelor · Kei Saito

Received: 30 June 2022 / Accepted: 18 October 2023 / Published online: 2 January 2024

Abstract The conventional production of nanocellulose from biomass demands multiple steps involving numerous chemicals like corrosive acids, bases, halogenated bleaching agents, and mechanical energy. This research aims to find a greener approach to producing nanocellulose particles from biomass. In nature, the brown rot fungi utilize iron complex and hydrogen peroxide to overcome the lignin boundary and approach cellulose in biomass. This fact encouraged us to use the same oxidative catalytic system on biomass in a one-pot process. Pinewood sawdust was taken as starting material, and the iron oxide, hydrogen peroxide oxidation system was applied with varying the concentration of hydrogen peroxide and the reaction time. In 6 h, a one-pot system obtained a 95% pure cellulose with an aspect ratio of 1–15 from pinewood sawdust. The yield of the process was very high, i.e., from the total cellulose content in pinewood, 85% of cellulose was recovered in this process. The degree of polymerization of the obtained cellulose product was 100 ± 20, with an aspect ratio of 1–20. The particles were sphere and ellipsoidal-shaped, with the majority having a diameter of 120–180 nm. It had a crystallinity of 81%, an increase of 26% crystallinity was observed compared to the untreated pinewood sawdust. These nanocellulose particles would be a promising material for different derivatizing reactions, with their high surface area (15.0 ± 0.5 m^2/g) and low degree of polymerization. This developed one-pot process has avoided using hazardous chemicals to produce nanocellulose particles.

Supplementary Information The online version contains supplementary material available at https://doi.org/10.1007/s10570-023-05573-2.

P. Vijay · K. Saito (✉)
School of Chemistry, Monash University, Clayton, VIC 3800, Australia
e-mail: saito.kei.1y@kyoto-u.ac.jp

V. S. Raghuwanshi · W. Batchelor
Department of Chemical and Biological Engineering, BioPRIA, Monash University, Melbourne, VIC 3800, Australia
e-mail: warren.batchelor@monash.edu

J. Ma
Monash X-Ray Platform and Department of Materials Science and Engineering, Monash University, Melbourne, VIC 3800, Australia

K. Saito
Graduate School of Advanced Integrated Studies in Human Survivability, Kyoto University, Higashi-Ichijo-Kan, Yoshida-Nakaadachicho 1, Sakyo-Ku, Kyoto 606-8306, Japan

Graphical abstract

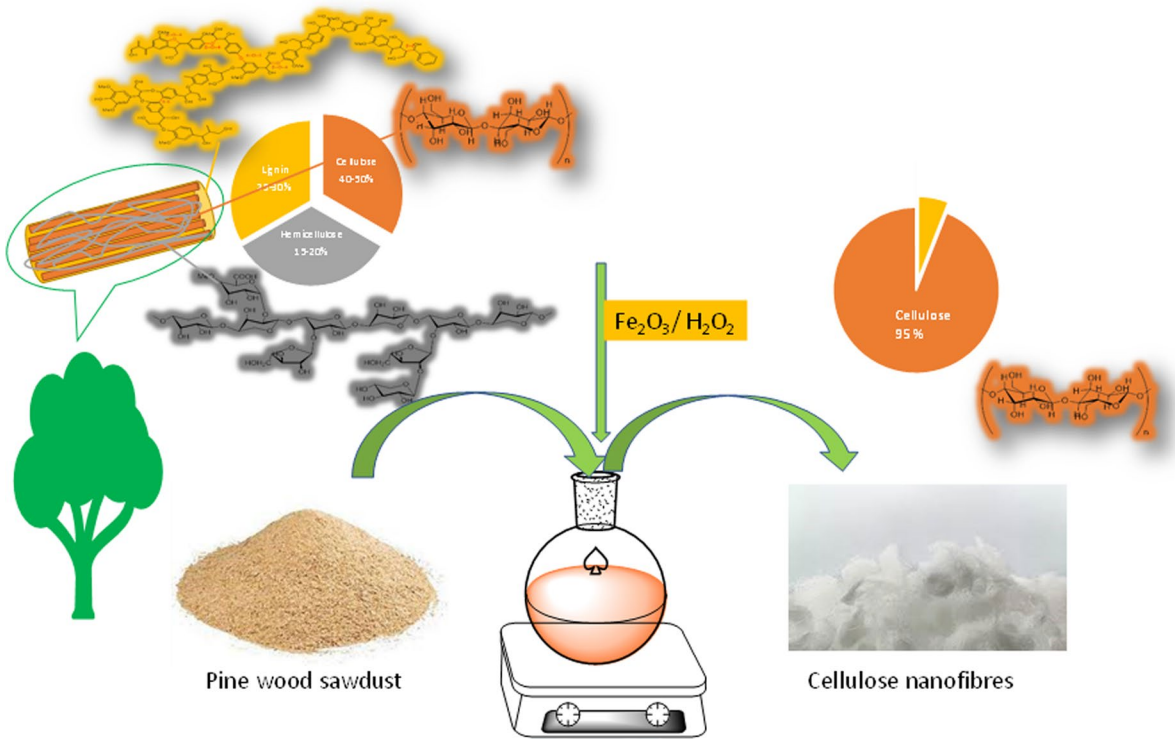

Keywords Green treatment · Non-hazardous materials · Non-halogenated materials · Biomass treatment · Fenton reagent · Nanocellulose

Abbreviations

NC	Nanocellulose
Fe_2O_3/H_2O_2	Iron oxide-hydrogen peroxide catalytic system
BEK cellulose	Bleached eucalyptus kraft cellulose
RB flask	Round-bottomed flask
DI water	Deionized water
NREL	National renewable energy laboratory
SEM	Scanning electron microscopy
DP	Degree of polymerization
CED	Cupriethylenediamine solution
XRD	X-ray diffraction

Introduction

The conventional process of producing nanocellulose (NC) with less non-cellulosic components from biomass involves three primary levels of treatment. Various pretreatment methods are the first level of treatment and are used to eliminate non-cellulosic components from the biomass. One of the methods is by using various hazardous chemicals (Fodil Cherif et al. 2020) such as acids, alkalis, lime, sulfur dioxide, organic solvents, and ionic liquids, to name a few. For example, the sulfite method of delignification involves the usage of sulfurous acid at elevated temperatures. Some alkalis used for the pretreatment are NaOH, KOH, $Ca(OH)_2$, hydrazine, and anhydrous ammonia (Kumar et al. 2020). For example, the kraft method of delignification involves the usage of an aqueous solution containing NaOH and Na_2S at

200 °C temperature (Agor et al. 2011; Bahera et al. 2014). Another method of pretreating biomass is the physicochemical method of steam explosion, where the biomass is treated with steam at high pressure and temperature. These pretreatments break the linkages between cellulose and non-cellulosic compounds (lignin and hemicellulose) to form a cellulose-rich fraction (Kumar et al. 2020).

Once the cellulose-rich fraction is obtained after the pretreatment of biomass, the bleaching process at the second level of treatment is conducted to remove the remaining lignin fractions. For this purpose, various bleaching agents are applied, such as sodium chlorite, sodium hypochlorite, and alkaline hydrogen peroxide (Sharma et al. 2020; Peltola et al. 2019; Dutra et al. 2018). As the final level of treatment, the bleached cellulose is chemically or/and mechanically treated to produce NC. This treatment can be achieved by using mechanical defibrillation such as refining, high-pressure homogenization, ball milling, grinding, and cryo-crushing, with and without chemical and enzymatic pretreatments such as TEMPO mediated oxidation, periodate-chlorite oxidation, carboxy-methylation, sulfonation, quarternization, acid hydrolysis, and cellulase treatments (Isogai et al. 2011; Liimatainen et al. 2012; Yarbrough et al. 2017; Mahmud et al. 2019).

Hence overall preparation of NC from lignocellulose involves many steps which deal with strong and hazardous chemicals (Nagarajan et al. 2021). These treatments negatively affect the process through the generation of toxic and hazardous wastes and high overall process expenses. Therefore, we need to develop a safer chemical process to produce NC.

In order to reduce the environmental footprints of existing chemical production processes, industries need to look for cleaner technologies. The use of environmentally friendly oxidants such as molecular oxygen and H_2O_2 are finding faster adaption to develop cleaner technology. H_2O_2 is used as an oxidant for producing chemicals such as hydrazine, phenol, adipic acid hydroquinone, etc. H_2O_2 is a preferred choice against halogenated oxidants in pulp and paper industries due to its lower environmental footprint, i.e. the only byproduct produced due to the H_2O_2 is water. (Goyal et al. 2022) However, the production of H_2O_2 is the main issue of concern as it demands high energy consumption and the usage of complicated solvent systems. Well-established industrial production of H_2O_2 is by Anthraquinone autoxidation (AO) process. In the AO process, 2-ethyl anthraquinol is oxidized by oxygen to corresponding quinone and H_2O_2. The anthraquinone produced is reduced back to anthraquinol with hydrogen using platinum, palladium or Raney nickel catalyst. The reaction is carried out using a mixture of organic solvents. Finally, the H_2O_2 is stripped from the organic solution with water in a counter-current column. The AO process suffers from numerous drawbacks, such as the cost and complexity of the solvent system to keep both reactant and the product in the solution, nonselective hydrogenation results in loss of quinone, deactivation of hydrogenation catalyst and elaborate treatments to remove degradation products. The AO process requires a large production plant. Significant efforts are being made to develop new cost-effective production technologies based on the direct oxidation of hydrogen to H_2O_2. Small-scale, on-site production of H_2O_2 is highly desirable to meet the requirement of pulp and paper industries. (Goyal et al. 2022; Jia et al. 2022).

In nature, microorganisms like fungi utilize iron complex and hydrogen peroxide to overcome the lignin barrier and other extractives of the lignocellulose to reach the cellulose (Arantes et al. 2012; Presley et al. 2018). This motivated us to study a similar method to remove non-cellulosic components from the lignocellulose. Our team successfully produced NC from cellulose, not biomass, using the iron oxide-hydrogen peroxide (Fe_2O_3/H_2O_2) catalytic system (Vijay et al. 2022). Bleached eucalyptus kraft cellulose (BEK cellulose) was taken as a starting material. The hydroxyl radicals produced in the reaction could depolymerize the cellulose, primarily at its amorphous region, to produce NC. Hence, we proved that the controlled oxidation of cellulose using the Fe_2O_3/H_2O_2 catalytic system could result in NC production.

The present investigation aimed to assess the same catalytic system (Fe_2O_3/H_2O_2) on biomass (pinewood sawdust). The main goal of this study is to determine whether it is possible to optimize the reaction condition in order to selectively remove non-cellulosic components from lignocellulose and defibrillate cellulose to NC with a high yield in a one-pot process.

The biomass used for this research is sawdust of pine stem wood. The catalytic system for this research is iron oxide (hematite, Fe_2O_3) and hydrogen peroxide (H_2O_2), which are very mild reagents, together

acting as a Fenton-like reagent to produce hydroxyl radicals. The hydroxy radicals have a very high oxidation potential (2.6 eV). The only byproducts in a Fenton-like reaction are water and carbon dioxide. The advantage of using hematite over other inorganic iron salts (like ferrous sulfate) is that there is no need to maintain the pH of the reaction mixture below pH 3. The Fenton process has been utilized to treat recalcitrant organics present in the paper and pulp mill effluents (Garcia-Segura et al. 2016; Kamali and Khodaparast 2015). To the best of the author's knowledge, Fenton-like reactions using Fe_2O_3 and H_2O_2 have never been used to isolate NC from lignocellulose in a one-pot process.

The first section of this article discusses the most suitable delignification conditions of pinewood that are required to obtain a product with a maximum cellulose content. FTIR and NREL methods are used to monitor the composition of the products. Then the products are characterized using NMR, XRD, TGA, SEM, BET methods, and method for determination of the degree of polymerization (DP).

Experimental section

Materials

Pinewood sawdust (biomass) was received from a local sawmill based in Melbourne, Australia. The received pinewood was dried in an oven at 40 °C for 48 h. Hydrogen peroxide (H_2O_2) solution 30wt% in water, iron (III) oxide (Fe_2O_3) powder (< 5 µm) were purchased from Sigma Aldrich. Paper filter "Advantec" 90 mm, grade no.2 used for the filtration was purchased from Labtek Pty Ltd.

One-pot treatment of pinewood sawdust

One-pot treatment of pinewood sawdust reactions using two different hydrogen peroxide concentrations, 20% and 30%, were investigated at different time intervals. For 20% hydrogen peroxide concentration, pinewood (5 g, oven-dried) was taken in a round-bottomed flask (RB flask) with 85 ml deionized water (DI water). First, 5 wt% (by weight of pinewood) of iron oxide Fe_2O_3 was added to the RB flask. The RB flask was stirred and sonicated for 10 min. The mixture was heated with stirring. Then, 85 ml of 30 wt% H_2O_2 was added to the mixture twice, first at the beginning of the reaction and next after 2 h of reaction, to make the total hydrogen peroxide concentration added to the reaction mixture 20%.

For 30% hydrogen peroxide concentration, pinewood (5 g, oven-dried) was taken in an RB flask with 125 ml of 30 wt% H_2O_2. In addition, 5 wt% (by weight of pinewood) of iron oxide Fe_2O_3 was added to the RB flask. The RB flask was stirred and sonicated for 10 min. The mixture was heated to 90 °C with stirring. After 2 h of reaction, another 125 ml of 30 wt% H_2O_2 was added. The reactions were carried out at different time intervals using two hydrogen peroxide concentrations.

The reaction mixture was cooled to room temperature and filtered. The separated solid product was taken in a beaker with 50 ml DI water, stirred for 5 min, and filtered. The catalyst remaining in the product was filtered through the filter paper, repeated stirring with water, and filtered three times to remove the maximum amount of catalyst. Finally, the product was dried in a freeze drier for two days and taken for further analysis. From the amount of product recovered from the reaction, the percentage of total solid recovered was calculated compared to the amount of pinewood taken (Table 1, column 12). Fig. 1 shows the starting material, Pinewood sawdust (Pine-0 h), and the product (Pine-30%-6 h).

Compositional analysis

Pinewood sawdust and the products were analyzed to find the compositions using the NREL (National Renewable Energy Laboratory) method, as described briefly below (Sluiter et al. 2010). All the measurements were carried out in triplicates.

Sample preparation for pinewood sawdust for the compositional analysis: Pinewood sawdust was passed through a Sieve shaker to separate the fractions of size between 180 and 400 µm. The sieved biomass was dried at 45 °C until a constant weight was obtained. This sieved, dried sawdust was taken for further analysis.

Ash content test: A known weight of the dried sample was heated at 575 °C in the muffle furnace for 24 h. The ash formed was then cooled in a desiccator and weighed. Percentage ash content was calculated.

Determination of extractives: A known weight of the sample was extracted with DI water, followed by

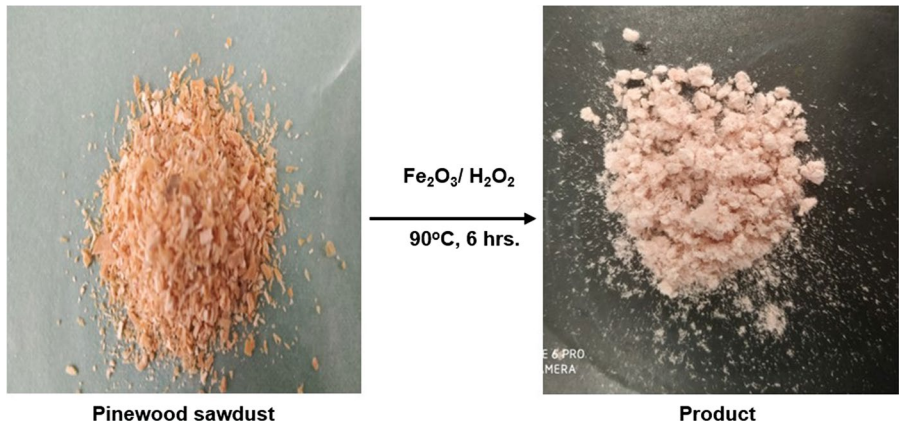

Fig. 1 Starting material (Pinewood sawdust) and the product (Pine-30%-6 h)

Table 1 Compositional analytical results of pinewood and products at different time intervals

Entry	Name	Yield (wt%)	Cellulose (%)	Lignin (%)		Hemicellulose (%)			Others (%)	
			Glucose	Insoluble	Soluble	Mannose	Xylose	Galactose	Ash	Extractive
1	Pine-0 h	–	42 ± 3	27 ± 2	1.3 ± 0.3	11.8 ± 0.2	5.7 ± 0.2	2.3 ± 0.1	0.1 ± 0.05	9 ± 1
2	Pine-20%-3 h	90 ± 2	45 ± 2	27 ± 1.5	1.3 ± 0.3	11.5 ± 0.1	5 ± 0.1	2 ± 0.1	0.3 ± 0.04	4 ± 1
3	Pine-20%-6 h	76 ± 3	60 ± 5	22 ± 2	3.6 ± 0.5	7.5 ± 1	4.3 ± 0.2	2 ± 0.1	0.3 ± 0.04	2 ± 0.5
4	Pine-20%-9 h	30 ± 2	87 ± 2	1 ± 0.5	4 ± 0.6	0	3 ± 0.3	0	0.3 ± 0.03	0
5	Pine-30%-3 h	80 ± 4	50 ± 5	24 ± 0.9	2 ± 0.2	11 ± 0.5	5 ± 0.2	2 ± 0.1	0.3 ± 0.05	4 ± 0.5
6	Pine-30%-6 h	38.5 ± 2	94.2 ± 1	0	5.5 ± 0.4	0	0	0	0.3 ± 0.03	0

ethanol using Soxhlet apparatuses. Extractive-free biomass was dried in an oven at 100 °C. The weight percentage of total extractives was determined.

Analysis of carbohydrate and lignin in biomass: Briefly, Extractive free biomass was hydrolyzed in two stages, firstly by using 72% H_2SO_4 and then with 4% H_2SO_4. The acid-insoluble fraction was utilized to determine the acid-insoluble lignin. The acid-soluble fraction was analyzed for acid-soluble lignin (by using the UV–Vis method) as well as total carbohydrates (using HPLC analysis).

Characterization methods

The percentage yields (mentioned in Table 1, column 3) of the products obtained in different conditions are calculated using the formula,

$$\text{Yield (wt\%)} = (\text{wt. of product} \div \text{wt. of pinewood taken for reaction}) * 100 \quad (1)$$

HPLC was conducted using an Agilent Infinity 1220 system coupled with a refractive index detector. A BioRad HPX-87P column was used for compositional analysis. The column was operated at 80 °C using deionized water at a constant flow of 0.7 ml min^{-1}. The calibration was performed using the values obtained by the range of monomeric sugars (glucose, mannose, xylose, galactose, arabinose). All the measurements were carried out in triplicate.

UV–Vis results were obtained using UV-1800 Shimadzu spectrophotometer. The UV–Vis was calibrated using the extracted acid-soluble lignin using the "Determination of Acid Soluble Lignin Concentration Curve by UV–Vis Spectroscopy" method. The percentage of acid-soluble lignin in hydrolyzed liquid at different time intervals were analyzed from its absorption value at 320 nm wavelength.

IR spectroscopy measurements were done using Agilent Cary 630, with 32 scans at a resolution of 8 cm^{-1}. The spectra were recorded in transmission mode in the region 4000–750 cm^{-1}. The baseline was created and subtracted by using the second derivative

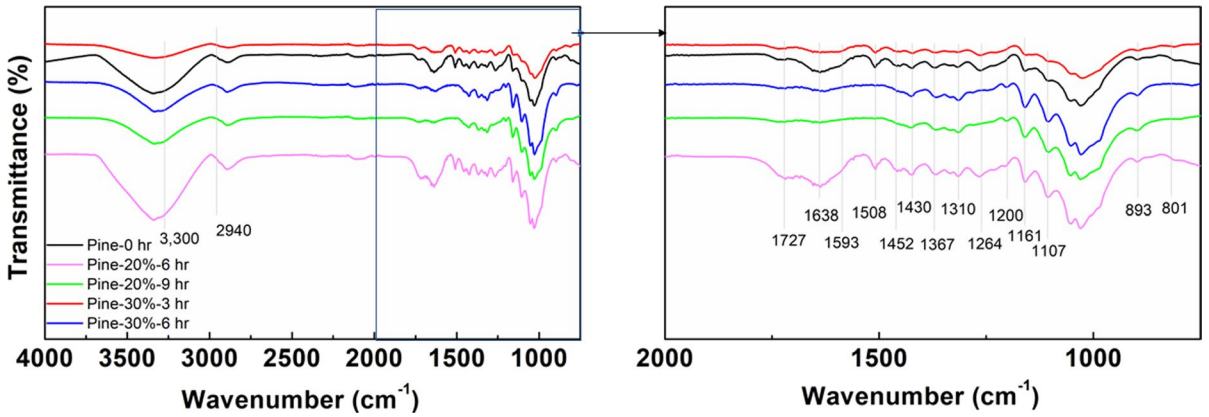

Fig. 2 IR spectra of Pine-0 h, Pine-20%-6 h, Pine-20%-9 h, Pine-30%-3 h, Pine-30%-6 h

method in the Peak Analyzer module of the Origin software.

Solid-state 13C NMR was measured using Bruker Avance spectrometer (Karlsruhe, Germany) equipped with a 7.05 Tesla magnet, operating at 75.4 MHz.

FEI Nova NanoSEM 450, equipped with a field-emission source at 5 kV, was used to perform scanning electron microscopy (SEM). The sample preparation for SEM was done by diluting the sample to 0.002 wt% and 0.001 wt% in ethanol and by pipetting 10 µl of the prepared sample onto carbon stubs. The air-dried sample was then coated with iridium for 2 nm thickness.

The degree of polymerization (DP) was determined by dissolving the sample in cupriethylenediamine (CED) solution and measuring the intrinsic viscosity. The DP values were determined using the Mark-Houwink-Sakurada equation,

$$[\eta] = 0.57 \times \mathrm{DP}. \quad (2)$$

where [ŋ] represents intrinsic viscosity (Zimmermann et al. 2010).

X-ray Diffraction (XRD) characterization was performed using a Bruker D8 Advance X-ray diffractometer with Cu Kα radiation of major wavelengths of Kα1 (0.15406 nm) and Kα2 (0.15444 nm) with generator voltage at 40 kV and current at 40 mA. Optics used included a Ni-filter, 2.5° Soller slits and an anti-scattering knife edge positioned 2 mm above the sample surface. The powder form samples were packed into a sample holder with a cavity of 2 mm depth to avoid X-ray transparency. XRD data were collected between 2θ angles of 5–60° using Lynxeye XE position-sensitive detector in 1D mode. A step size of 0.03° was used. All samples were run with a divergence angle at 0.3° and a dwell time of 2 s per step.

The relative crystallinity index was calculated using Segal's method, as explained in the supporting information (French 2014, 2020).

Thermogravimetric analysis (TGA) was performed on a Mettler TGA/DSC1 STAR system, ranging from 40 to 800 °C. The heating rate was fixed to 20 °C/min under nitrogen flow.

The surface area of the product was measured by calculating the adsorbing amount of N_2 (BET method) at various relative vapor pressures. The samples were prepared by vacuum drying for 24 h at 110 °C. The analysis was recorded by a TriStar II 3020 (Micromeritics, U.S.A.) analyzer.

Results and discussion

The reaction of pinewood with Fe_2O_3/H_2O_2 catalyst

The reactions were conducted at 90 °C temperature and varying time intervals of 3, 6, and 9 h. Reactions were done using two different H_2O_2 concentrations, 20% and 30%. All the products obtained were preliminarily analyzed using IR spectroscopy, later by the NREL method (compositional analysis), to determine the most suitable reaction condition. When 20% H_2O_2 is used, products of 6 h reactions showed the IR spectra with all the peaks corresponding to pinewood (IR

spectra of original pinewood and 6 h reaction product can be seen in Fig. 2, labelled as Pine-0 h and Pine-20%-6 h). When 30% H_2O_2 was used, a 3 h reaction product (Pine-30%-3 h) showed the IR transmittance also as same as Pine-0 h.

The IR spectra of Pine-0 h, Pine-20%-6 h, and Pine-30%-3 h have the transmittance at wavenumber, 3400–3200 cm^{-1}, which is assigned to the –OH stretching alcoholic and phenolic stretching groups involved in hydrogen bonding in hemicellulose cellulose and lignin; 2942 cm^{-1}, which corresponds to C–H stretching of methyl, methylene or methane groups in lignin. The signals near 3500 cm^{-1} and between 1640 and 1630 cm^{-1} correspond to the residual water molecules. Further, the IR spectrums, Pine-0 h and Pine-20%-6 h, Pine-30%-3 h are showing transmittance at 1682, 1638 cm^{-1}. These two values correspond to the unconjugated and conjugated C=O stretch of lignin molecules. Transmittance value 1593 and 1508 cm^{-1} represents C=C, C=O stretch in lignin and C=C stretch of the aromatic ring in lignin. Transmittance peak at 1727 cm^{-1}corresponds to the C=O group of unconjugated ketone and carboxylic groups in hemicellulose. Further, the peak at 1264 cm^{-1} gives the lignin aromatic ring vibration, and 1227 cm^{-1} gives the C–C, C–O vibrations in lignin. A tiny peak at 867 cm^{-1} corresponds to glycosidic linkage in hemicellulose (Ong et al. 2020; Kaffashsaie et al. 2021).

In comparison, all peaks mentioned above corresponding to lignin and hemicellulose have either wholly disappeared or drastically reduced in the case of the 9 h reaction using 20% H_2O_2 (Pine-20%-9 h) and the 6 h reaction using 30% H_2O_2 (Pine-30%-6 h) spectrums. Also, all the transmittance peaks of Pine-20%-9 h and Pine-30%-6 h strongly emphasize the presence of a maximum of cellulose in those samples with the prominent peaks of cellulose; they are transmittance bands at 893 cm^{-1} (glycosidic linkage vibration), 1031 cm^{-1} (C–O stretching), 1107,1161 and 1058 cm−1 are assigned to pyranose ring skeletal vibration. 1200 cm^{-1} (–OH bending), 1310 cm^{-1} (CH_2 wagging vibration), 1367 cm^{-1} (C–H bending), and 1430 cm^{-1} are due to the CH_2 asymmetric bending vibration of cellulose I (native cellulose), 2900 cm^{-1} (C–H stretching) in crystalline order of cellulose. These observations suggest that the product has native cellulose I structure, and the treatment did not alter the cellulose internal arrangement.

The disappearance of lignin and hemicellulose stretching and vibration peaks indicate that most of the hemicellulose and lignin have been removed in the case of Pine-20%-9 h and Pine-30%-6 h products.

Hence if 30% H_2O_2 is used, a 6 h reaction is sufficient to remove non-cellulosic material from pinewood, whereas 20% H_2O_2 needs 9 h to do the same.

The points which can be drawn from FTIR analysis are the preservation of cellulose I structure in the product. After most of the lignin is removed from the wood, the resulting cellulose product remains unoxidized. The observations drawn from FTIR reports were confirmed by conducting the compositional analysis using the NREL method of compositional analysis of pinewood (Pine-0 h) and all the products obtained at different reaction intervals. The results acquired are shown in the table below.

As can be seen in Table 1 above, the NREL method of compositional analysis shows that untreated pinewood (Table 1, entry 1) had 42 ± 3% of cellulose (considering that glucose content is the result of cellulose hydrolysis)) content in it. Additionally, it has 29 ± 2.3% total lignin (combined acid-insoluble lignin and acid-soluble lignin) and a total of 19.8 ± 0.5% of hemicellulose (combined mannose, xylose and galactose contents). The ash content and total extractives present in pinewood were 0.1 ± 0.05% and 9 ± 1%, respectively. When 20% hydrogen peroxide was used, the cellulose (glucose) content in the extracted products kept increasing with the increase in reaction time, with the decrease in lignin and hemicellulose content. When the reaction was continued for 9 h, the product Pine-20%-9 h had 87 ± 2% cellulose (glucose), with around 5% lignin and 5% hemicellulose. The total product yield recovered from the reaction was 30 ± 2 wt% of the total pinewood taken. When 30% hydrogen peroxide was used, the same trend was observed, provided that, within 6 h of reaction, the product Pine-30%-6 h had 95% cellulose (glucose) with around 5.5% soluble lignin in it. The total solid recovered at the end of the process, which is the yield of the reaction, was 38.5 ± 2 wt% of the total pinewood taken. Hence, from the Pine-0 h, which had 42 ± 3% cellulose, Pine-30%-6 h had recovered 38.5 ± 2 wt% of the product with 95% cellulose within 6 h of reaction. Comparatively, Pine-30%-6 h had a better yield (38.5 ± 2 wt%, with respect to starting material taken) than that of the product, Pine-20%-9 h (30 ± 2 wt%). Hence, using

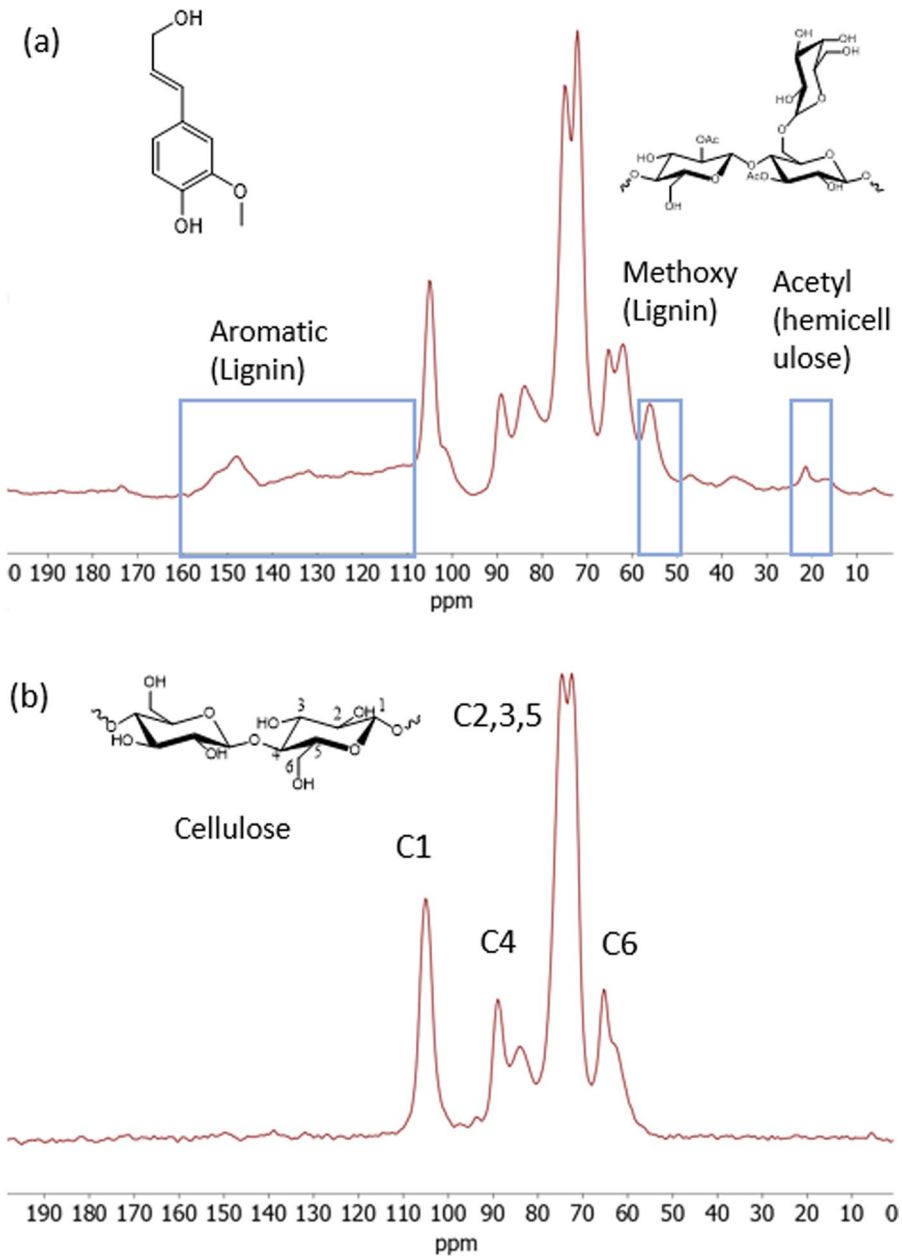

Fig. 3 C^{13} NMR of **a** Pine-0 h, **b** Pine-30%-6 h product

30% H_2O_2 for a 6 h reaction was the best condition for the reaction. HPLC chromatogram of acid hydrolyzed Pine-0 h and Pine-30%-6 h are given in supplementary data Fig. S1. Pine-0 h had peaks corresponding to glucose, mannose, xylose and galactose, whereas Pine-30%-6 h showed a single peak corresponding to glucose.

The ash content of all the products (Table 1, entry 2 to entry 6) is approximately 0.2% more than that of the pinewood. This increase in ash content is due to the residual Fe_2O_3 remaining in the products. Hence, the product's color is a pale pink, as seen in Fig. 1.

The product Pine-30%-6 h was taken for further analysis.

C-13 NMR spectra

The C-13 solid-state NMR of pinewood, Pine-0 h (Fig. 3a), and Pine-30%-6 h (Fig. 3b) are given below. Spectra (a) from Pine-0 h has the chemical

shifts in the region, 110–170 ppm, corresponding to the lignin aromatic carbons. Also, the carbon of the methoxy group of lignin appeared as a peak at a chemical shift of 55 ppm in the spectra. Cellulose peaks were also presented in the spectra from Pine-0 h, which are peaks in the chemical shift of 102–108 ppm for C1, 80–92 ppm for C4, and 57–67 ppm for C6 carbon. The chemical shift at 20 ppm corresponds to the hemicellulose acetyl group was also detected. In the case of spectra (b), only the peaks attributed to cellulose were visible. All the aromatic peaks of the lignin in the region 110–170 ppm and methoxy carbon of lignin in the region 55 ppm have disappeared in spectra (b). Also, the typical hemicellulose acetyl peak at 20 ppm entirely disappeared in spectra (b). These observations confirm the removal of non-cellulosic materials from the pinewood in the Pine-30%-6 h product; only pure cellulose remains in the product. This absence of carbons in a new environment suggests that the process doesn't alter the basic chemical structure of cellulose.

XRD

The XRD pattern of Pine-0 h and Pine-30%-6 h with 2Theta values at 14–17, 22.5 and 34.2 (Cu anode, WL = 1.5406 Å) are assigned to the cellulose I diffraction planes (1–10) (or 110), 200, and 004, respectively (French 2014; Tarchoun et al. 2020; Nishiyama et al. 2002; Wada et al. 2001). The XRD patterns are provided in the supporting information in Fig. S3 and Fig. S4. Thus, it is observed that the Fe_2O_3/ H_2O_2 system is not altering the cellulose I allomorph.

The relative crystallinity index (CI) was calculated by the Segal Crystallinity Index method (Segal et al. 1959). A baseline was subtracted from the XRD data (Fig. S3 for Pine-0 h and Fig. S4 for Pine-30%-6 h). The CI was calculated by taking the intensity of the crystalline (I_{cr}) peak centered at 22.5° and the intensity of the amorphous (I_{am}) peak at 18.9°. Details of the calculations are provided in the supporting information Table S1. The calculated CI for the Pine-0 h is 55%, and for the Pine-30%-6 h is 81%. (Macrae et al. 2008).

The evaluation of the crystallinity index using the Segal method shows an increase of 26% of crystallinity in Pine-30%-6 h compared to Pine-0 h.

This higher crystallinity index can be explained by the removal of amorphous hemicelluloses and lignin from the wood, a decrease in the content of amorphous domains in cellulose, as well as an increase in the number of intra- and intermolecular hydrogen bonds of cellulose.

As discussed in our previous work (Vijay et al. 2022), the used reagent (Fe_2O_3/ H_2O_2) attacks the amorphous domains of cellulose followed by the hydrolytic cleavage of their glycosidic bonds, which leads to the formation of highly ordered crystallites. This crystallinity index value is comparable to the microcrystalline cellulose obtained by acid hydrolysis of bleached pulp (El-Sakhawy and Hassan 2007).

Previously, different experimental methods, instruments and data analysis techniques were used to evaluate cellulose's crystallinity. Park et al. (2010) calculated the crystallinity of cellulose by solid-state ^{13}C NMR method and compared it with the existing XRD-based methods. The Rietveld refinement method for XRD can bring further accuracy in the crystallinity measurement, as mentioned by Driemeier and Calligaris (2011).

Rietveld refinement for the XRD patterns was performed by using Topas Academic v7 (Coelho AA, 2018) with pdf files from ICDD PDF 4 Organics 2013 (as mentioned in supporting information) for both I-β and amorphous. A fundamental parameters approach (Coelho and Cheary 1992) was used to describe instrument contribution to the peak shape. The D8 Advance diffractometer was calibrated with NIST standard 660c LaB_6, and the fundamental parameters approach was found to be suitable for defining the instrument's peak shape.

Crystallite size was calculated based on the integral breadth of diffraction peaks by using the Scherrer equation. (Scherrer P. 1918; French and Santiago Cintrón. 2013).

Rietveld refinement of the XRD pattern for the untreated pinewood, Pine-0 h, can be found in supporting information, Fig. S3. The crystallite size calculated based on the integral breadth is 1.85(17) nm, and lattice parameters *a* (Å), *b* (Å) and *c* (Å) are 7.90(4), 8.01(5) and 10.50(7) respectively.

Rietveld refinement of the XRD pattern for the treated pinewood, Pine-30%-6 h, can be found in supporting information, Fig. S4. The crystallite size calculated based on the integral breadth is 3.13(9) nm,

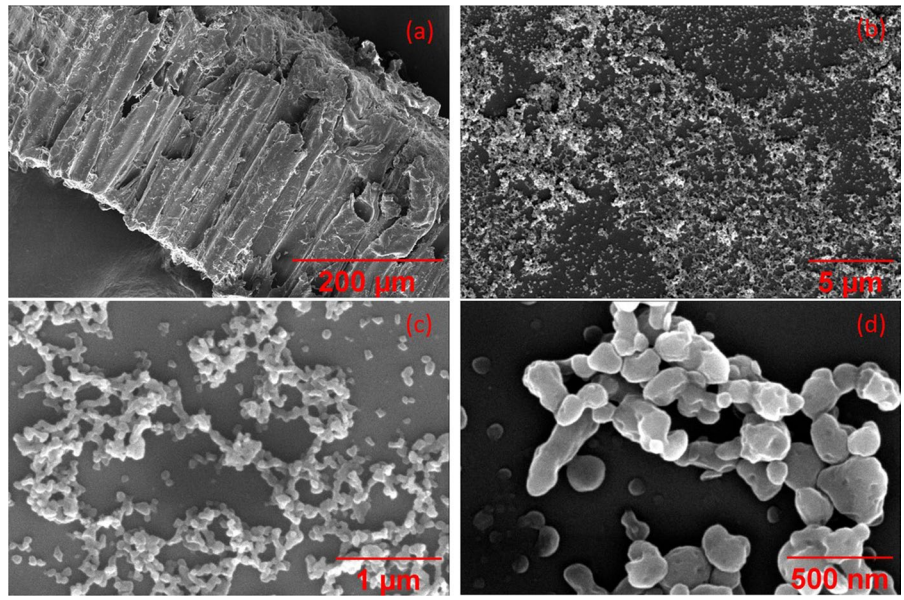

Fig. 4 SEM images of **a** Pine-0 h, **b** Pine-30%-6 h sample in 0.002% concentration. **c**, **d** show the Pine-30%-6 h of 0.001% concentration

and lattice parameters *a* (Å), *b* (Å) and *c* (Å) are 7.87(2), 7.95(2) and 10.62(3) respectively.

It can be found that the crystallite size shrank along *a* and *b* directions whereas it increased along the lattice parameter *c* in the case of Pine-30%-6 h as compared to Pine-0 h.

SEM analysis

SEM images of Pine-0 h and the Pine-30%-6 h at different concentrations are given in Fig. 4. Pine-0 h can be seen in, Fig. 4a, which has sheets of lignocellulose of more than 300 µm in length and 100 µm in thickness packed together.

Figure 4b shows the Pine-30%-6 h of 0.002% concentration. Figure 4c, d show Pine-30%-6 h of 0.001% concentration. In Fig. 4b, c highly broken particles arranged in a web-like arrangement aggregated in some areas and spread as particles in some areas.

In Fig. 4d and Fig. S5, sphere and ellipsoidal-shaped particles are 120–180 nm in diameter, with some smaller particles below 100 nm in diameter and a few bigger particles of up to 350 nm in diameter. The diameter of the particles in Fig. 4d is measured and displayed in supporting information in Fig. S5. The cellulose particles with the above-mentioned particle size can be called NC particles, as explained in the literature (Carvalho et al. 2021).

The above observations suggest that the Fe_2O_3/H_2O_2 catalytic system, in 6 h duration, breaks the pinewood sawdust of size 180–400 µm drastically to nanometer size cellulose particles.

As shown in Table 1 entry 6, these nano-sized particles are composed of 95% cellulose. Also, XRD data confirms the improvement in the crystallinity of the particles comparing to its starting material. So, it can be postulated that the catalytic system attacks the less crystalline hemicellulose and lignin in the pinewood; finally, the catalytic system attacks the amorphous region of cellulose to break the cellulose glycosidic bonds and forms nanometer-sized particles.

DP

DP of the products Pine-20%-9 h and Pine-30%-6 h (Table 1, entries 4 and 6 respectively) are analyzed. Both products have a high percentage of cellulose and very little lignin in them. The DP of both products was in the range of 100 ± 20.

Surface area measurement

Surface area measurement by nitrogen adsorption of Pine-30%-6 h revealed that the surface area was

15.0 ± 0.5 m^2/g. These values closely match the surface area of the previously reported NC (Guo and Catchmark 2012). In addition, they report the surface area of the cotton, which was 1.6 ± 0.2 m^2/g, has increased drastically to 11–16 m^2/g after treating it with H_2SO_4/HCl hydrolysis to produce NC.

The increased surface area of obtained NC has the potential for surface grafting of various polymers for the development of valuable composites.

TGA

The thermogravimetric analysis of Pine-0 h and the product, Pine-30%-6 h, is displayed in Supplementary data, Fig. S2. Pinewood sample DTG curve showed three degradation peaks at 240, 290 and 350 °C. These correspond to hemicellulose, cellulose and lignin decompositions, respectively. According to the reported TGA values of biomass, hemicellulose decomposes at lower temperatures (180–340 °C) than cellulose (230–450 °C) and lignin (> 350 °C) (Mishra and Mohanty 2018). In the Pine-30%-6 h product, only one decomposition peak is observed at 265 °C. The complete removal of hemicellulose and lignin attributes the reason for only the cellulose degradation peak in the TGA of the product, Pine-30%-6 h. The thermal stability of the product after the treatment slightly decreased due to the drastic decrease in the DP of the product, as discussed in the earlier research to obtain delignified biomass. (Kohli et al. 2020).

Comparison between other conventional methods of NC synthesis

Many delignification methods have been reported in the literature. These methods can comprise, for example, multi-step process using ionic liquids (Kohli et al. 2020), halogenated bleaching agents (Kaffashsaie et al. 2021), and alkaline treatments. Pure cellulose obtained after the delignification process is mainly subjected to acid hydrolysis at elevated temperatures to obtain NC (Chirayil et al. 2014). Many strong acids are employed, namely, 72% H_2SO_4, Conc. HCl, Conc. HNO_3, CH_3COOH etc. The resulting NC have residual sulfate or phosphate groups attached to the surface. Along with the usage of multi-step processes and corrosive chemicals, another disadvantage of these processes is the low yield of the NC produced at the end of the process (Wu et al. 2021).

On the other hand, enzymatic hydrolysis is considered an environmentally friendly option compared to the acid hydrolysis method for NC preparation. However, the drawback of this process is the low yield and the slow kinetics of the process (Alonso-Lerma et al. 2021).

Out of all these reported methods, our method shows the upper hand for the efficient removal of non-cellulosic materials to produce 95% cellulose and the formation of NC in a one-pot process using very mild reagents. Additionally, the high yield of 85% (of total cellulose in the pinewood taken for reaction) is a very promising outcome of this process.

The FTIR and NMR analyses confirm that the chemical structure of the native cellulose has not changed after the treatment with Fe_2O_3/H_2O_2 system. In addition, X-ray diffraction analysis confirms that the native crystalline allomorph of cellulose, cellulose I, also remained unchanged after such treatment. So, the treatment with Fe_2O_3/H_2O_2 did not alter the chemical and crystalline structure of cellulose.

TEMPO oxidation results in nanofibers, whereas the Fenton oxidation results in nanoparticles. The distinction between the two nanoproducts arises from the differing oxidation mechanisms employed. TEMPO-oxidised nanofibers are formed through the initial oxidation of cellulose fibre's surface hydroxy groups into carboxylate groups. The application of mild mechanical force induces electrostatic repulsion between these carboxylate groups, resulting in the formation of nanofibers. In our current research, the Fenton reagent is used to generate OH radicals, which effectively break down cellulose fibres into nanometer-sized particles. The mechanism is detailed in our previous study (Vijay et al. 2022).

According to previously reported literature, NC are fine, crystalline particles isolated from natural fibers. NC have many outstanding properties like hydrophilicity, water insolubility, nontoxicity, biodegradability and renewability. These features made them employed in several applications, such as cosmetics (thickeners, binders), pharmaceuticals (carriers and tablet media binders, absorbents), food (stabilizers, emulsifiers and fat substituents) and cosmetic industries (hair conditioner, dyes, shampoos, toothpaste) as it forms a colloidal dispersion in water (Heinze et al. 2018). Additionally, NC are also proven to be a suitable starting

Table 2 Comparing characteristics between the acid hydrolysis method (Hafid et al. 2021; Haldar and Purkait. 2020; Trache et al. 2017) and Fe_2O_3/H_2O_2 method

Entry	Acid hydrolysis method	Fe_2O_3/H_2O_2 method (this research)
1	Multi-step methods to separate non-cellulosic compounds first and then use acid hydrolysis on it	Single-step method, which removes all non-cellulosic compounds and produces NC
2	Usage of many hazardous chemicals in the entire process	Very mild reagent with only side product is water and CO_2
3	The yield is low (30–50%)	Very high yield (85%)
4	High crystallinity (70–80)	High crystallinity (81%)
5	Dimension (60–100 aspect ratio)	Dimension (1–20 aspect ratio)
6	Purity depends on the pretreatment methods	High purity, 95% cellulose
7	Surface area (11–16 m^2/g)	Surface area (15 m^2/g)
8	Addition of an anionic group during the process	No change in the chemical structure of cellulose after the treatment

material for derivatization reaction, as they still represent cellulose polymer, with sufficiently low viscosity to handle the quasi-homogeneous reaction systems. NC are a very promising starting material for many stimuli-responsive polymers grafting to a surface abundance of –OH groups, which favors their surface modification. Therefore, NC and their polymer composites can have a promising application potential. In this regard, several degradation steps were established to prepare low DP cellulose (Mailand et al. 2011; Tarchoun et al. 2019). Thus, the NC developed in this research has tremendous potential to be used in many applications with its low DP and high purity, as mentioned above.

The yield and the purity of cellulose obtained in this treatment are superior to the many other research reported in the literature (Barana et al. 2016; Jiao et al. 2016), where they use many toxic chemicals in multi-step processes to separate cellulose from lignocellulose (Tarchoun et al. 2019). These observations manifest the highly effective eco-friendly method applied in this research.

The table below gives a gist of comparable factors of the process and product developed in this research vs acid hydrolysis process of NC preparation: (Table 2)

Conclusion

We developed a promising one-pot extraction of NC particles from pinewood using a very mild reagent, Fe_2O_3/H_2O_2. The catalytic system used in this study removed all the non-cellulosic constituents of lignocellulose and produced NC particles with 95% pure cellulose content. The FTIR, and NMR spectra confirm that NC particle chemical structure is not influenced by the treatment given to the pine wood. The morphological analysis by SEM showed that the product obtained had an aspect ratio in the range of 1–20. The particles were sphere and ellipsoidal-shaped, with most of them having a diameter of 120–180 nm. Further, the product exhibited typical cellulose I allomorph, with a crystallinity of around 81% providing evidence that the Fe_2O_3/H_2O_2 reagent selectively removed the amorphous components of pinewood without altering its allomorph. Furthermore, the high yield of the product emphasizes the great potential of this Fe_2O_3/H_2O_2 catalytic reagent to replace conventional acid hydrolysis to obtain low DP, high pure, crystalline cellulose materials.

This process has avoided many steps involving various acid and base hydrolysis, halogenated bleaching methods, and harmful chemicals to separate lignin and hemicellulose from lignocellulose and produce NC. Thus, this work gives a sustainable process to produce low DP NC particles from biomass in one pot.

Acknowledgements The authors gratefully acknowledge the funding of the Australian Research Council (ARC) and Processing Advance Lignocellulosics (PALS) [grant number-IH170100020]. The authors also acknowledge the Monash school of chemistry, Monash X-ray Platform, and Monash Centre for Electron Microscopy to use facilities.

Author contributions All authors contributed to the study's conception and design. Material preparation, data collection and analysis were performed by PV, VR, JM. The first draft of the manuscript was written by PV and all authors commented

on previous versions of the manuscript. All authors read and approved the final manuscript.

Funding This work was supported by funding of the Australian Research Council (ARC) and Processing Advance Lignocellulosics (PALS) [grant number- IH170100020].

Availability of data and materials The data supporting this study's findings are available in this article's supporting information. In addition, other raw experimental data is available on request.

Declarations

Competing interests The authors declare no competing interests.

Conflict of interest The authors have no relevant financial or non-financial interests to disclose.

Ethics approval There was no ethical content in preparing this manuscript.

Consent to participate All authors consented to participate in this work.

Consent for publication All authors consented to publish this work.

References

Agbor VB, Cicek N, Sparling R, Berlin A, Levin DB (2011) Biomass pretreatment: fundamentals toward application. Biotechnol Adv 29:675–685. https://doi.org/10.1016/j.biotechadv.2011.05.005

Alonso-Lerma B, Larraza I, Barandiaran L, Ugarte L, Saralegi A, Corcuera MA, Perez-Jimenez R, Eceiza A (2021) Enzymatically produced cellulose nanocrystals as reinforcement for waterborne polyurethane and its applications. Carbohydr Polym 254:117478. https://doi.org/10.1016/j.carbpol.2020.117478

Arantes V, Jellison J, Goodell B (2012) Peculiarities of brown-rot fungi and biochemical Fenton reaction with regard to their potential as a model for bioprocessing biomass. Appl Microbiol Biotechnol 94:323–338. https://doi.org/10.1007/s00253-012-3954-y

Barana D, Salanti A, Orlandi M, Ali DS, Zoia L (2016) Biorefinery process for the simultaneous recovery of lignin, hemicelluloses, cellulose nanocrystals and silica from rice husk and Arundo donax. Ind Crops Prod 86:31–39. https://doi.org/10.1016/j.indcrop.2016.03.029

Behera S, Arora R, Nandhagopal N, Kumar S (2014) Importance of chemical pretreatment for bioconversion of lignocellulosic biomass. Renew Sust Energy Rev 36:91–106. https://doi.org/10.1016/j.rser.2014.04.047

Carvalho JPF, Silva ACQ, Silvestre AJD, Freire CSR, Vilela C (2021) Spherical cellulose micro and nanoparticles: a review of recent developments and applications. Nanomaterials 11:2744. https://doi.org/10.3390/nano11102744

Chirayil CJ, Mathew L, Thomas S (2014) Review of recent research in nono cellulose preparation from different lignocellulosic fibres. Rev Adv Mater Sci 37:20–28

Coelho AA (2018) TOPAS and TOPAS-academic: an optimization program integrating computer algebra and crystallographic objects written in C++. J Appl Cryst 51:210–218. https://doi.org/10.1107/S1600576718000183

Coelho A, Cheary RW (1992) A fundamental parameters approach to X-ray line-profile fitting. J Appl Cryst 25:109–121. https://doi.org/10.1107/S0021889891010804

Driemeier C, Calligaris GA (2011) Theoretical and experimental developments for accurate determination of crystallinity of cellulose I materials. J Appl Crystallogr 44:184–192. https://doi.org/10.1107/S0021889810043955

Dutra ED, Santos FA, Alencar BRA, Reis ALS, de Souza Rd FR, da Silva Aquino KA, Morais MA Jr, Menezes RSC (2018) Alkaline hydrogen peroxide pretreatment of lignocellulosic biomass: status and perspectives. Biomass Convers Biorefin 8:225–234. https://doi.org/10.1007/s13399-017-0277-3

El-Sakhawy M, Hassan ML (2007) Physical and mechanical properties of microcrystalline cellulose prepared from agricultural residues. Carbohydr Polym 67:1–10. https://doi.org/10.1016/j.carbpol.2006.04.009

Fodil Cherif M, Trache D, Brosse N, Benaliouche F, Tarchoun AF (2020) Comparison of the physicochemical properties and thermal stability of organosolv and kraft lignins from hardwood and softwood biomass for their potential valorization. Waste Biomass Valor 11:6541–6553. https://doi.org/10.1007/s12649-020-00955-0

French AD (2014) Idealized power diffraction patterns for cellulose polymorphs. Cellulose 21:885–896. https://doi.org/10.1007/s10570-013-0030-4

French AD (2020) Increment in evolution of cellulose crystallinity analysis. Cellulose 27:5445–5448. https://doi.org/10.1007/s10570-020-03172-z

French AD, Santiago Cintrón M (2013) Cellulose polymorphy, crystallite size, and the segal crystallinity index. Cellulose 20:583–588. https://doi.org/10.1007/s10570-012-9833-y

Garcia-Segura S, Bellotindos LM, Huang Y-H, Brillas E, Lu MC (2016) Fluidized-bed Fenton process as alternative wastewater treatment technology—a review. J Taiwan Inst Chem Eng. 67:211–225. https://doi.org/10.1016/j.jtice.2016.07.021

Goyal R, Singh O, Agrawal A, Samanta C, Sarkar B (2022) Advantages and limitations of catalytic oxidation with hydrogen peroxide: from bulk chemicals to lab scale process. Catal Rev Sci Eng 64:229–285. https://doi.org/10.1080/01614940.2020.1796190

Guo J, Catchmark JM (2012) Surface area and porosity of acid hydrolyzed cellulose nanowhiskers and cellulose produced by Gluconacetobacter xylinus. Carbohydr Polym 87:1026–1037. https://doi.org/10.1016/j.carbpol.2011.07.060

Hafid HS, Omar FN, Zhu J, Wakisaka M (2021) Enhanced crystallinity and thermal properties of cellulose from rice husk using acid hydrolysis treatment. Carbohydr Polym 260:117789. https://doi.org/10.1016/j.carbpol.2021.117789

Haldar D, Purkait MK (2020) Micro and nanocrystalline cellulose derivatives of lignocellulosic biomass: a review on synthesis, applications and advancements. Carbohydr Polym 250:116937. https://doi.org/10.1016/j.carbpol.2020.116937

Heinze T, El Seoud OA, Koschella A (2018) Cellulose derivatives: synthesis, structure, and properties; Springer, 2018

Isogai A, Saito T, Fukuzumi H (2011) TEMPO-oxidized cellulose nanofibers. Nanoscale 3:71–85. https://doi.org/10.1039/C0NR00583E

Jia Y, Bai Y, Chang J, Zhai Y, Zhang T, Ren K, Hong J (2022) Life cycle assessment of hydrogen peroxide produced from mainstream hydrogen sources in China. J Clean Prod 352:131655. https://doi.org/10.1016/j.jclepro.2022.131655

Jiao Y, Wan C, Qiang T, Li J (2016) Synthesis of superhydrophobic ultralight aerogels from nanofibrillated cellulose isolated from natural reed for high-performance adsorbents. Appl Phys A 122:1–10. https://doi.org/10.1007/s00339-016-0194-5

Kaffashsaie E, Yousefi H, Nishino T, Matsumoto T, Mashkour M, Madhoushi M, Kawaguchi H (2021) Direct conversion of raw wood to tempo-oxidized cellulose nanofibers. Carbohydr Polym 262:117938. https://doi.org/10.1016/j.carbpol.2021.117938

Kamali M, Khodaparast Z (2015) Review on recent developments on pulp and paper mill wastewater treatment. Ecotoxicol Environ Saf 114:326–342. https://doi.org/10.1016/j.ecoenv.2014.05.005

Kohli K, Katuwal S, Biswas A, Sharma BK (2020) Effective delignification of lignocellulosic biomass by microwave assisted deep eutectic solvents. Bioresour Technol 303:122897. https://doi.org/10.1016/j.biortech.2020.122897

Kumar V, Pathak P, Bhardwaj NK (2020) Waste paper: an underutilized but promising source for nanocellulose mining. Waste Manag 102:281–303. https://doi.org/10.1016/j.wasman.2019.10.041

Liimatainen H, Visanko M, Sirvio JA, Hormi OE, Niinimaki J (2012) Enhancement of the nanofibrillation of wood cellulose through sequential periodate–chlorite oxidation. Biomacromolecules 13(5):1592–1597

Macrae CF, Bruno IJ, Chisholm JA, Edgington PR, McCabe P, Pidcock E, Rodriguez-Monge L, Taylor R, van de Streek J, Wood PA (2008) Mercury CSD 2.0-new features for the visualization and investigation of crystal structures. J Appl Crystallogr 41:466–470. https://doi.org/10.1107/S0021889807067908

Mahmud MM, Perveen A, Jahan RA, Matin MA, Wong SY, Li X, Arafat MT (2019) Preparation of different polymorphs of cellulose from different acid hydrolysis medium. Int J Biol Macromol 130:969–976. https://doi.org/10.1016/j.ijbiomac.2019.03.027

Meiland M, Liebert T, Heinze T (2011) Tailoring the degree of polymerization of low molecular weight cellulose. Macromol Mater Eng 296:802–809. https://doi.org/10.1002/mame.201000424

Mishra RK, Mohanty K (2018) Pyrolysis kinetics and thermal behavior of waste sawdust biomass using thermogravimetric analysis. Bioresour Technol 251:63–74. https://doi.org/10.1016/j.biortech.2017.12.029

Nagarajan K, Ramanujam N, Sanjay M, Siengchin S, Surya Rajan B, Sathick Basha K, Madhu P, Raghav GA (2021) Comprehensive review on cellulose nanocrystals and cellulose nanofibers: pretreatment, preparation, and characterization. Polym Compos 42:1588–1630. https://doi.org/10.1002/pc.25929

Nishiyama Y, Langan P, Chanzy H (2002) Crystal structure and hydrogen-bonding system in cellulose 1β from synchrotron X-ray and neutron fibre diffraction. J Am Chem Soc 124(31):9074–9082. https://doi.org/10.1021/ja025 7319

Ong HC, Chen W-H, Singh Y, Gan YY, Chen C-Y, Show PL (2020) A state-of-the-art review on thermochemical conversion of biomass for biofuel production: a TG-FTIR approach. Energy Convers Manag 209:112634. https://doi.org/10.1016/j.enconman.2020.112634

Park S, Baker JO, Himmel ME, Parilla PA, Johnson DK (2010) Cellulose crystallinity index: measurement techniques and their impact on interpreting cellulase performance. Biotechnol Biofuels 3:1–10. https://doi.org/10.1186/1754-6834-3-10

Peltola H, Immonen K, Johansson LS, Virkajärvi J, Sandquist D (2019) Influence of pulp bleaching and compatibilizer selection on performance of pulp fiber reinforced PLA biocomposites. J Appl Polym Sci 136:47955. https://doi.org/10.1002/app.47955

Presley GN, Panisko E, Purvine SO, Schilling JS (2018) Coupling secretomics with enzyme activities to compare the temporal processes of wood metabolism among white and brown rot fungi. Appl Environ Microbiol 84:e00159-e218. https://doi.org/10.1128/AEM.00159-18

Scherrer P (1918) Bestimmung der Größe und der inneren Struktur von Kolloidteilchen mittels Röntgenstrahlen: Nachrichten von der Gesellschaft der Wissenschaften zu Göttingen. Mathematisch-Physikalische Klasse, Berlin, pp 98–100. http://eudml.org/doc/59018

Sharma N, Bhardwaj NK, Singh RBP (2020) Environmental issues of pulp bleaching and prospects of peracetic acid pulp bleaching: a Review. J Clean Prod 256:120338. https://doi.org/10.1016/j.jclepro.2020.120338

Sluiter JB, Ruiz RO, Scarlata CJ, Sluiter AD, Templeton DW (2010) Compositional analysis of Lignocellulosic feedstocks. 1. Review and description of methods. J Agric Food Chem 58:9043–9053. https://doi.org/10.1021/jf1008023

Tarchoun AF, Trache D, Klapötke TM, Derradji M, Bessa W (2019) Ecofriendly isolation and characterization of microcrystalline cellulose from giant reed using various acidic media. Cellulose 26:7635–7651. https://doi.org/10.1007/s10570-019-02672-x

Tarchoun AF, Trache D, Klapötke TM, Krumm B, Khimeche K, Mezroua AA (2020) Promising energetic biopolymer based on azide-functionalized microcrystalline cellulose: synthesis and characterization. Carbohydr Polym 249:116820

Trache D, Hussin MH, Haafiz MKM, Thakur VK (2017) Recent progress in cellulose nanocrystals: sources and

production. Nanoscale 9(5):1763–1786. https://doi.org/10.1039/C6NR09494E

Vijay P, Batchelor W, Saito K (2022) One-pot treatment of cellulose using iron oxide catalysts to produce nanocellulose and water-soluble oxidized cellulose. Carbohydr Polym 282:119060. https://doi.org/10.1016/j.carbpol.2021.119060

Wada M, Okano T, Sugiyama J (2001) Allomorphs of native crystalline cellulose I evaluated by two equatorial *d*-spacings. J Wood Sci 47:124–128. https://doi.org/10.1007/BF00780560

Wu L, Tian F, Sun J (2021) On the use of cellulose nanowhisker as reinforcement in all-cellulose composite membrane from corn stalk. J Appl Polym Sci 138:50206. https://doi.org/10.1002/app.50206

Yarbrough JM, Zhang R, Mittal A, Vander Wall T, Bomble YJ, Decker SR, Himmel ME, Ciesielski PN (2017) Multifunctional cellulolytic enzymes outperform processive fungal cellulases for coproduction of nanocellulose and biofuels. ACS Nano 11:3101–3109. https://doi.org/10.1021/acsnano.7b00086

Zimmermann T, Bordeanu N, Strub E (2010) Properties of nanofibrillated cellulose from different raw materials and its reinforcement potential. Carbohydr Polym 79:1086–1093. https://doi.org/10.1016/j.carbpol.2009.10.045